Electrically controllable microlens array fabricated by anisotropic phase separation from liquid-crystal and polymer composite materials

Hee-Su Ji and Jae-Hoon Kim

Department of Physics, Hallym University, Chunchon, Kangwon-Do 200-702, Korea

Satyendra Kumar

Department of Physics, Kent State University, Kent, Ohio 44242

Received December 17, 2002

Anisotropic phase separation has been used to fabricate an electrically switchable microlens array from nematic liquid crystals. Nematic liquid-crystal-based microlens arrays have been built with diameters of ~400 μm and natural focal lengths as small as 1.6 mm. The focal length of each microlens in the array can be changed in milliseconds by an applied electric field. These devices, which have no internal substructures to scatter light, offer higher efficiency and greater light throughput than polymer dispersed devices. © 2003 Optical Society of America

OCIS codes: 230.3020, 230.4600.

With the advancements in computing and communications technology, there is a growing and critical need for real-time reconfigurable optical elements such as fast optical switches, beam-steering (e.g., diffractive gratings) and wave-front-shaping (e.g., microlens arrays) devices for use in high-density data storage, optical interconnects, and beam-modulating and energy-directing devices. The ability to control the action of these devices electrically is a key requirement. Various attempts have been made to construct real-time reconfigurable microlens arrays from liquid crystals,[1,2] which perform real-time optical interconnection in optical computing and photonic switching circuits. The technology required for achieving such active microlenses is fundamentally different from the technology for passive elements that use surface-relief structures.[3–5] Methods used in previous studies to build electrically controllable microlens arrays have included (i) a combinations of a passive solid-state lens array and a liquid-crystal (LC) modulator[6] and (ii) a gradient refractive-index profile of a LC produced with an axially symmetric electric field generated by specially designed electrode patterns.[1,2]

A method of preparing LC devices was developed recently that uses one-dimensional anisotropic phase separation of a LC from its solution in a polymer, which yields adjacent layers of LC and polymer known as phase-separated composite organic films (PSCOFs).[7] These PSCOFs are unique structures and exhibit electro-optical properties that are not observed in devices prepared by conventional methods or by other phase-separation techniques such as polymer dispersion and polymer stabilization. Because the PSCOF technology has the advantages of ease of fabrication, mechanical ruggedness, and flexibility of fine tuning of the optical path length, it is suitable for devices in optical communication. In this Letter we report a simple method for fabricating LC-based switchable microlens arrays by using a three-dimensional anisotropic phase-separation technique is modified from the PSCOF method.

The materials used in this study are a commercial nematic LC (E31 from Merck Chemical Company) and a photocurable prepolymer (NOA-65 from Norland). The ordinary and extraordinary refractive indices of LC E31 at room temperature are 1.535 and 1.762, respectively, at 589.3 nm, and the refractive index of the cured NOA65 prepolymer is 1.524. Cell spacing is controlled with the use of glass fiber or bead spacers of 5–25-μm diameter. To align the LC, we make cells by using substrates coated with rubbed films of poly(vinyl alcohol). A solution of the LC and the prepolymer, in a weight ratio of 60:40, is introduced into the cell by capillary action in the isotropic phase. The cells are exposed to UV light of $\lambda = 350$ nm to initiate polymerization. A xenon (Oriel Model 6269) 200-W lamp is the source of UV light.

In the simplest case, when a cell filled with a mixture of LC and prepolymer is exposed to normally incident UV light, an intensity gradient in the z direction perpendicular to the cell is produced as a result of absorption of UV light by the mixture. The intensity gradient causes anisotropic phase separation[8,9] along the z direction. The use of a suitable mask during UV exposure produces additional intensity gradients in the xy plane of the cell. Monomers in the high-intensity region near the UV source undergo polymerization first, and monomers in the low-intensity region diffuse to the high-intensity region to maintain their relative concentration and join the polymerization reaction.[10] The LC molecules are immiscible in and are expelled from the polymer. Therefore the phase separation is anisotropic in three dimensions. Depending on the shape of the photomask, we can fabricate complex microstructures of pure LCs of various shapes, sizes, and director orientations.

Figure 1 shows the fabrication process for a microlens array. We use a surface-relief array of hemispheres as a photomask. The surface-relief structure is placed on one of the glass substrates without the poly(vinyl alcohol) alignment layer. The cell with the mixture of a LC and a prepolymer is

0146-9592/03/131147-03$15.00/0

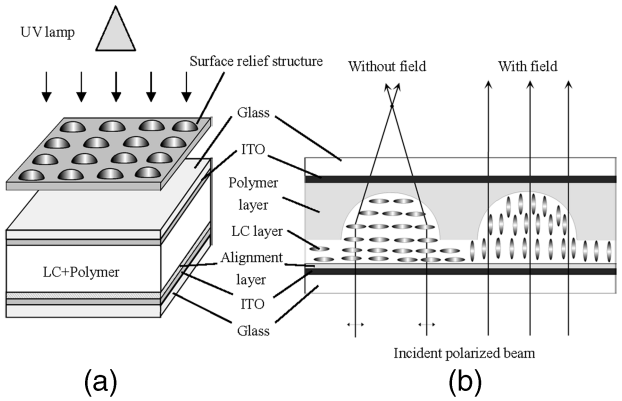

Fig. 1. Schematic diagrams of (a) the fabrication setup and (b) the resultant structure for two operating states of a nematic LC microlens array. The hemispheric surface-relief array was from UV-curable polymer. ITO, indium tin oxide.

irradiated with UV light for ~10 min. A second exposure is performed for 5 min without the relief array to fully harden the polymer. During this process the LC molecules that remain in the polymer network after first UV exposure are expelled from the polymerized volume. Because of the thickness-dependent absorption, an UV intensity gradient is created across the circular areas, which in turn causes anisotropic phase separation that results in the highest LC concentration in the middle of the shadow. On completion of polymerization, an array of three-dimensional plano–convex structures, which act as microlenses, is obtained as shown in Fig. 1(b). The natural focal length f of a microlens can be calculated from $f = R(n_{\mathrm{LC}} - n_{\mathrm{p}})$, where R is the radius of curvature of the lens's surface and n_{LC} and n_{p} are the effective LC and polymer indices of refraction, respectively. One can change the focal length by changing the effective value of n_{LC} with the help of an applied electric field. The effective value of n_{LC} depends on the polarization of the incident light. When the polarization is parallel to the director, the light beam sees the extraordinary refractive index ($n_{\mathrm{LC}} = n_e = 1.762$) of LC E31 in the absence of an applied field, and $f = 4.2R$. When the applied field exceeds a certain threshold value, the LC director begins to be reoriented along the field, and the incident beam sees a component of ordinary refractive index ($n_{\mathrm{LC}} = n_o = 1.535$) of LC E31. At the highest fields the focal length becomes as large as $91R$.

Figure 2 shows polarizing microscopic textures of the cell after UV exposure with and without an applied field. Clearly, very regular internal structures are formed, as shown in Fig. 2(a). A set of concentric circular fringes is visible in the regions that were under the surface-relief hemisphere, indicating a continuous variation of the optical path length from the center to the edge. The circular rings are surrounded by relatively uniform regions. One can get a uniformly dark state outside the circular regions [Figs. 2(b)] by rotating the cell between crossed polarizers.

We determine the focal length of these microlenses by mounting the cell on a micrometer motion translation stage illuminated with a collimated He–Ne laser beam (632.8 nm) from one side. Light passing through the lens is collected by an imaging lens and detected by a CCD camera. To measure the focal length, we first focus the imaging lens on the microlens's surface and then we move the lens array toward or away from the imaging lens to find the focal point. Figure 3 shows the focusing properties of the laser beam through the lens. The polarization of the incident beam is parallel to the direction of the LC director. Figure 3(a) shows the image of the beam focused by one microlens with no applied field. The microlens acts as a plano–convex lens with focal length f of 1.7 mm. The light-intensity profile measured at the focal point is shown in Fig. 3(b). When we apply 3 V, the beam is defocused [Fig. 3(c)] and then refocused at a distance of 3.7 mm [Fig. 3(d)].

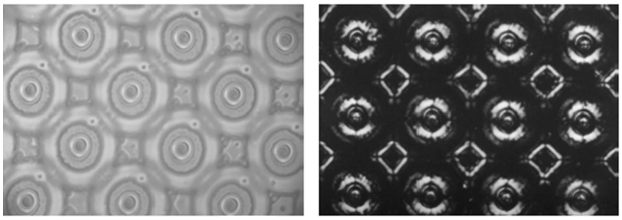

Fig. 2. Microscopic textures of a microlens array under a polarizing microscope with no voltage applied. The rubbing direction is rotated (a) 45° and (b) 0° with respect to one of the crossed polarizers. Concentric rings of different colors signify changing optical thicknesses, and areas of uniform shading outside the lenses indicate cell uniformity.

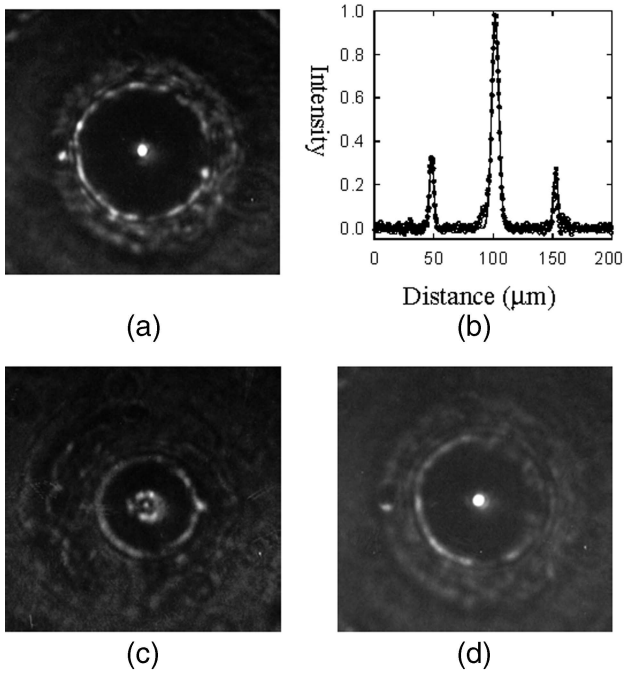

Fig. 3. Focusing properties of the laser beam through the lens: (a) focused beam image at 1.7 mm with no voltage applied, (b) light-intensity profile at the focal point, (c) defocused beam image with 3 V at 1.7 mm, (d) refocused beam image with 3 V at 3.7 mm.

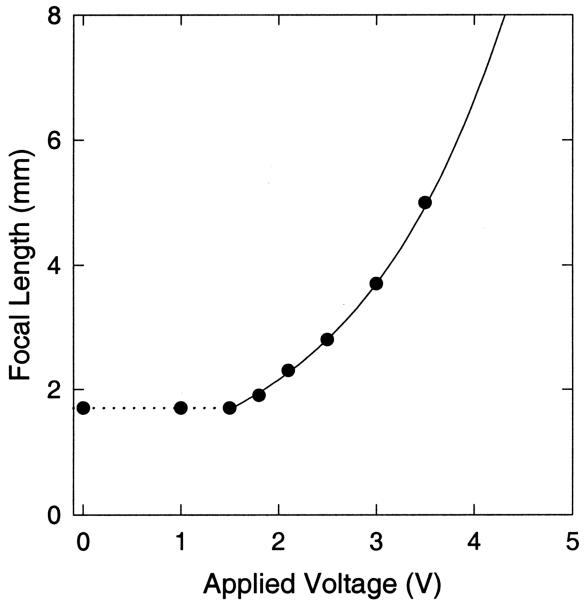

Fig. 4. Dependence of the microlen's focal length on voltage. The focal length increases quadratically for fields higher than the threshold value of 1.5 V.

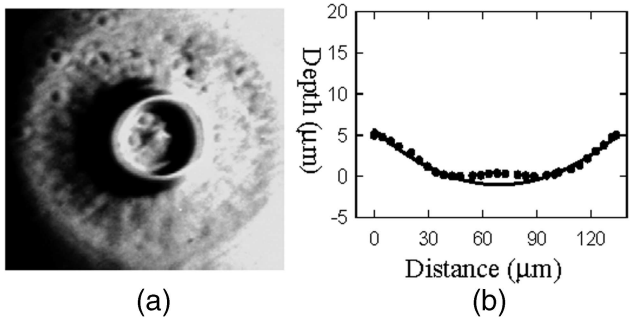

Fig. 5. (a) Microscopic structure and (b) depth profile of one of the microlenses. The curve in (b) is a fit to determine the radius of curvature, $R = 381 \pm 20$ μm, and the diameter, ~ 150 μm.

From the measured dependence of the focal length on the applied voltage as shown in Fig. 4, it is clear that f depends quadratically on the field beyond a threshold value of 1.5 V. The switching times from focusing to nonfocusing states and back are ~30 and 130 ms, respectively. However, higher speeds can be achieved with a ferroelectric LC. We also confirm the value of f by using a microscope to measure the magnification of an object (the number 15 on a reticule; 0.37 mm $\times$ 0.41 mm in size), its distance from the lens, and the position of the image.

To determine the geometrical shape and the value of R of these structures we pried open a cell and washed away the LC with hexane. Figures 5(a) and 5(b) show the polymer structure under a microscope in the reflective mode and the shape profile of the central region, respectively. The radius of curvature of the crater-like central region was 381 $\pm$ 20 mm, as determined from a least-squares fit to a circle, represented by the solid curve in Fig. 5(b). Natural focal length f was 1.6 $\pm$ 0.1 mm, in good agreement with the measured value of 1.7 mm.

We control the curvature of the LC–polymer interface by changing the cell thickness, the relative diffusion rates of LC and polymer, and the rate of polymerization. It is possible to fabricate microlenses of different focal lengths. With proper selection of the LC and polymer materials it is possible to fabricate a converging ($n_{\mathrm{LC}} > n_{\mathrm{p}}$) or a diverging ($n_{\mathrm{LC}} < n_{\mathrm{p}}$) lens or a lens that changes from converging to diverging ($n_e < n_{\mathrm{p}} < n_o$). The microlens density and placement in the array can be controlled with the use of appropriate photomasks. The ability to address each lens individually with any of the well-known matrix-addressing schemes commonly used in LC display devices makes these lenses highly versatile.

We have proposed and demonstrated a new method for the fabrication of an electrically controllable two-dimensional microlens array. The lens array was fabricated by anisotropic phase separation from a composite of an UV-curable polymer and liquid crystal. The focal length varies with the applied voltage as well as with the concentration of LCs and the sample thickness. Because of the internal structure, the lenses possess the capability of withstanding high mechanical stress and are likely to posses high efficiency and transmission. Furthermore, they can be prepared with flexible, thin, and low-weight substrates. They should prove to be valuable in focused beam steering and as active fiber star couplers for high-density optical communications, parallel interconnects for neural networks, and optical limiters as well as in other military applications.

This research was supported in part by Korea Research Foundation grant KRF-2001-005-DP0191 and by the National Science Foundation's Science and Technology Center for Advanced Liquid Crystalline Optical Materials grant DMR-89-20147. J.-H. Kim's e-mail address is jhkim@hallym.ac.kr.

References

1. T. Nose and S. Sato, Liq. Cryst. **5,** 1425 (1989).
2. T. Nose, S. Masuda, S. Sato, J. Li, L. Chien, and P. Bos, Opt. Lett. **22,** 351 (1997).
3. M. N. F. Borrelli and O. L. Morse, Appl. Opt. **27,** 476 (1988).
4. M. Wang and H. Su, Opt. Lett. **23,** 876 (1998).
5. M. Fritze, M. Stern, and P. Wyatt, Opt. Lett. **23,** 141 (1998).
6. K. Rastani, C. Lin, and J. S. Patel, Appl. Opt. **31,** 3046 (1992).
7. V. Vorflusev and S. Kumar, Science **283,** 1903 (1999).
8. T. Qian, J.-H. Kim, S. Kumar, and P. L. Taylor, Phys. Rev. E **61,** 4007 (2000).
9. V. Krongauz, E. Schmelzer, and R. Yohannan, Polymer **32,** 1654 (1991).
10. X. Wang, Y. Yu, and P. L. Taylor, J. Appl. Phys. **80,** 3285 (1996).